

# Analysis and Design of a Novel Power Supply for Mobile Robots\*

J. W. Raade, H. Kazerooni, T. G. McGee

*Department of Mechanical Engineering  
University of California, Berkeley  
Berkeley, CA 94720*

*Corresponding Author: H. Kazerooni, kazerooni@me.berkeley.edu*

**Abstract** - We have developed a novel device to supply hydraulic power for anaerobic mobile robotic systems. This power source is capable of operation in environments with no oxygen, such as underwater and space. The design, unlike the internal combustion engine, produces power on demand, eliminating idling when there is no load on the system. Steam and oxygen are the only byproducts of this power supply. This monopropellant-powered free piston hydraulic pump (FPHP) was designed as a human scale (1.0 to 3.0 kW) power supply. The FPHP utilizes high concentration hydrogen peroxide, which decomposes into hot gas when exposed to a catalyst, as the monopropellant energy source. Energy is extracted from the hydrogen peroxide and transferred directly to hydraulic fluid by expanding the hot decomposition gas in an integrated piston/cylinder arrangement. Based upon a specific power and specific energy analysis using a Ragone plot, the performance of the FPHP potentially exceeds that of a battery based hydraulic power supply for short operation times.

**Index Terms** – monopropellant; free piston; mobile robotics; anaerobic power; Ragone plot

## I. INTRODUCTION

The lack of compact, efficient, and lightweight power sources impedes the realization of mobile robotic devices that operate autonomously for periods of hours. While technology for mobile robotic platforms, communication, information processing, and automation has accelerated, similar breakthroughs for power sources have not kept pace. Mobile robotic systems require energetic autonomy with no tether connecting the machine to its power supply. Hence, the power supply must be portable and have a long operation time. Along with the engine itself, the fuel and fuel tank mass must be taken into account when evaluating a potential power system design. These requirements make the power supply performance the limiting factor in mobile robotic autonomy.

Anaerobic power supplies have an additional constraint placed on their design. Unlike air-breathing robotic applications, which have the ability to consume fuel oxidizer directly from the atmosphere, anaerobic applications must carry their oxidizer with them, greatly reducing the effective specific energy of their fuel. Gasoline, for example, requires 14.6 kg of air for one kilogram of fuel to burn at a stoichiometric mixture [1].

A free piston internal combustion engine represents a

possible solution to the need for a potent power supply. Various studies have produced theoretical simulations of hydrocarbon powered free piston engines [2-4]. However, [5] describes the only known free piston engine capable of practical operation. Free piston engines are not widespread due to the significant design problems presented by the creation of an operational free piston engine. Without good compression, thorough fuel/air mixing, and properly timed ignition, a free piston engine will stall. Monopropellants such as hydrazine or hydrogen peroxide enable a unique solution to the characteristic difficulties of a free piston engine, eliminating the problems of fuel/air mixing, compression and ignition, startup, and idling. Monopropellants have the additional advantage of requiring no separate oxidizer to release their energy. Researchers have recently explored the use of hydrogen peroxide to move pneumatic actuators [6]. The free piston hydraulic pump (FPHP) described in this work integrates a monopropellant based robotic power supply and a free piston pump, two concepts not previously realized in a single system.

The FPHP represents a concept that may be developed into a feasible mobile robotic power supply capable of energetic autonomy. A monopropellant powered FPHP is capable of operation independent of the atmosphere with no separate oxidizer, making operation possible in such anaerobic environments as underwater, space, and oxygen deprived buildings. This paper builds off the work in [7] and [8] and presents an evaluation of the FPHP in terms of specific energy and specific power using a Ragone plot [9]. First, this paper describes the concept of a monopropellant powered FPHP as well as the energetics of monopropellants. Next, a dynamic analysis of the FPHP is presented. Then the hardware design problems are presented along with their solutions. Finally, the FPHP is evaluated in terms of specific energy and specific power.

## II. THE CONCEPT

In spite of its limited practicality to date, the free piston concept is a simple, elegant format for a hydraulic power supply. In contrast to the standard reciprocating engine, a free piston engine extracts work from hot gas by directly harnessing linear motion of the piston and pressurizing the hydraulic fluid, resulting in an integrated engine/pump design. Fig. 1 shows a cross sectional diagram of the final design concept of the FPHP. Its overall length from catalyst bed to catalyst bed is approximately 68 cm (27 inches). The catalyst beds use fine silver mesh to decompose the hydrogen peroxide. The FPHP

\* This project was funded in part by the Office of Naval Research grant number N000-14-98-1-0669, the National Science Foundation, and the Department of Defense.

has no actuated hydraulic or exhaust valves, only passive one-way check valves for the hydraulic fluid and exhaust ports for the hot gas.

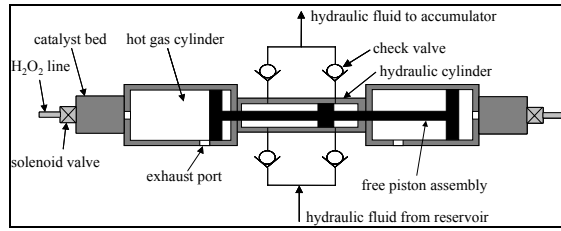


Figure 1: Double acting free piston concept.

The operation of the FPHP begins with the injection of high-pressure hydrogen peroxide into the left catalyst bed by opening the left solenoid valve. The hydrogen peroxide decomposes into steam and oxygen as it passes through the left catalyst bed. These hot gases expand within the left hot gas cylinder and force the free piston assembly to the right. The free piston's movement pumps hydraulic fluid at high pressure from the right chamber of the hydraulic cylinder while simultaneously drawing in low pressure fluid from the reservoir into the left chamber of the hydraulic cylinder. During this stroke the upper right and lower left check valves are open while the upper left and lower right check valves remain closed. The hot gases expand until the hot gas piston uncovers the left exhaust ports, at which point the gases vent to the atmosphere and the free piston stops moving. The right solenoid valve then opens to begin the cycle on the opposite side of the FPHP, moving the left hot gas piston from the exhaust port toward the cylinder head and compressing the gas in the left cylinder. This cycle is the same as the left-hand process. During operation, the free piston assembly moves right and left, resulting in a pulsating flow of hydraulic fluid from the reservoir to the accumulator.

The overall performance goal for a proof-of-concept FPHP was to achieve an average continuous power output of 2.2 kW (3.0 horsepower) by pumping hydraulic fluid at 6.9 MPa (1000 psi) and 19 liters/min (5.0 gallons/min). All pressures are expressed as gauge pressure. The mass of the FPHP was not optimized since its purpose was to demonstrate the concept of a novel mobile robotic power supply, not to embody a field-ready device. In order to achieve the desired hydraulic power output and flow rate, the FPHP was designed to operate at ten cycles per second. One cycle was defined as a complete stroke of the free piston assembly to the right followed by a complete stroke to the left. To minimize monopropellant consumption, the FPHP needed to maximize the computed conversion efficiency,  $\eta_{conv}$ , defined as the output hydraulic work divided by the chemical energy put into the system:

$$\eta_{conv} = \frac{W_{out}}{E_{in}} = \frac{P_{avg} V}{Q_{LHV} m_{HP}} \quad (1)$$

where  $P_{avg}$  is the average hydraulic pressure over one stroke,  $V$  is the volume of the hydraulic fluid expelled during one stroke,  $Q_{LHV}$  is the lower heating value of the hydrogen peroxide, and  $m_{HP}$  is the mass of the hydrogen peroxide injected for one stroke.

The final dimensions of the FPHP, driven by the aforementioned performance goals, were determined from an iterative process with the theoretical model and simulation of the FPHP as developed in [7]. For example, a smaller hot gas cylinder bore resulted in slower peak free piston speeds, which eased hydraulic sealing but also resulted in lower power output. During the design process, possible bore and stroke sizes of the hot gas cylinder as well as relative diameters of the hot gas and hydraulic pistons were evaluated with the simulation in order to arrive at the final values. The final design theoretically produces the required power output while maintaining a relatively low peak free piston speed of 8.0 meters per second (m/s). The area ratio between the hot gas piston and the hydraulic piston is 6.5, resulting in a pressure amplification in the hydraulic fluid. The pressure amplification facilitates the venting of the hot gas at a lower pressure, extracting more work from the hot gas while still maintaining an average hydraulic pressure near 6.9 MPa.

### III. MONOPROPELLANT ENERGETICS

Monopropellants spontaneously decompose into hot gas when brought into contact with a catalyst, requiring no oxidizer to release energy. This characteristic provided a unique solution to the typical problems of a free piston engine. There was no need for compression or mixing with air to provide power, eliminating the need to properly control a spark and regulate a compression ratio. The lack of a flywheel, a disadvantage for a gasoline or diesel powered free piston engine, provided the benefit of power on demand for the monopropellant powered FPHP. The FPHP could be started and stopped intermittently, since the monopropellant could be injected and decomposed at any desired time. Continuous operation was achieved by injecting enough monopropellant each cycle to move the free piston the length of its stroke.

Hydrogen peroxide ( $H_2O_2$ ) was selected as the monopropellant for this project since it is readily available in a pure, highly concentrated form from several commercial sources. Additionally, hydrogen peroxide produces only steam and oxygen as decomposition products, which are non-toxic.

Specific energy is defined as the total energy content of a fuel or a power supply system divided by its mass, expressed in terms of megajoules per kilogram (MJ/kg). Pure hydrogen peroxide releases 2.9 MJ/kg of energy at standard temperature and pressure conditions [10]. This is the higher heating value of hydrogen peroxide, which indicates that the water in the products is in liquid form. The lower heating value indicates that the water is in vapor form in the exhaust, and provides a more realistic measure of the available energy in the monopropellant since the exhaust is hot gas containing water vapor. The lower heating value of hydrogen peroxide, 1.6 MJ/kg, is considerably lower than that of hydrocarbon fuels, which are approximately 44 MJ/kg. For anaerobic operations, however, this large difference is justified since gasoline would require a separate oxidizer as well as a means to mix and combust the fuel and oxidizer.

### IV. DYNAMIC ANALYSIS OF FPHP

Once the conceptual design of the FPHP was finalized, a dynamic model was required to evaluate the behavior of the system [7]. The dynamics of the FPHP are driven by the

motion of the free piston assembly (FPA) which is governed by

$$\sum F = m\ddot{x} = A_g(P_{gH} - P_{gL}) - A_f(P_{fH} - P_{fL}) - F_{fric} \quad (2)$$

where  $m$  denotes the mass of the FPA,  $\ddot{x}$  is its linear acceleration and  $\sum F$  is the sum of the forces acting on the FPA, which are illustrated in Fig. 2. No force is modeled on the back faces of the hot gas pistons since both are well vented to atmosphere.

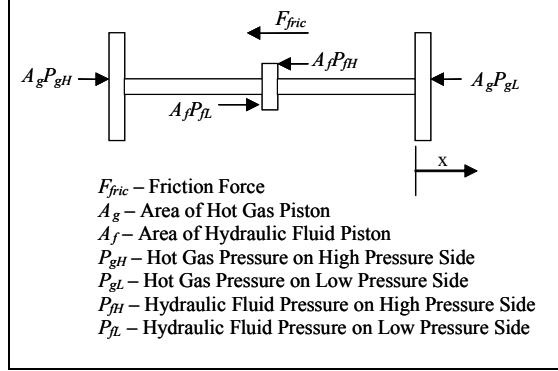


Figure 2: Free body diagram of FPA.

The hot gas cylinder of the FPHP is modeled as a control volume with the hot gases entering at the adiabatic decomposition temperature ( $T_{ad}$ ) of the hydrogen peroxide. Since each stroke occurs in a relatively short time, very little heat is lost through the cylinder walls. The process is therefore assumed to be adiabatic. The energy balance for an adiabatic control volume with entering gas is

$$\dot{m}_i h_i - \dot{W} = \frac{d}{dt} E_{system} \quad (3)$$

where  $\dot{m}_i$  is the mass flow rate of hot gas into the control volume,  $h_i$  is specific enthalpy of the gas,  $\dot{W}$  is the rate of work done by the system on the surroundings, and  $E_{system}$  is the total energy of the control volume system. The rate of work can be calculated from the FPA velocity,  $\dot{x}$ , the hot gas pressure,  $P_{gH}$ , and the hot gas piston area,  $A_g$ .

$$\dot{W} = A_g P_{gH} \dot{x} \quad (4)$$

Since the kinetic and gravitational potential energies of the hot gas are negligible, the total energy of the system is equal to the internal energy of the hot gas. This internal energy, assuming an ideal gas approximation, can be calculated from the gas temperature,  $T_g$ , the total mass of the gas,  $m_g$ , and the specific heat of the gas,  $c_v$ .

$$E_{system} = m_g c_v T_g \quad (5)$$

The mass of the gas can be also be expressed as the product of its density,  $\rho$ , the hot gas piston area, and FPA displacement.

$$m_g = \rho A_g x \quad (6)$$

Assuming ideal gas properties, the specific heat can be calculated from the gas constant,  $R$  and the specific heat ratio  $k$ , which are known properties of the gas. Using the ideal gas assumption for the specific heat and inserting (6) into (5) yields

$$E_{system} = \frac{A_g x \rho R T_g}{k-1} \quad (7)$$

Using the ideal gas law on (7) yields

$$E_{system} = \frac{A_g x P_{gH}}{k-1} \quad (8)$$

Differentiating (8) with respect to time,

$$\frac{d}{dt} E_{system} = \frac{A_g}{k-1} (\dot{x} P_{gH} + x \dot{P}_{gH}) \quad (9)$$

The enthalpy of the incoming hot gas can be determined from its temperature.

$$h_i = c_p T_{ad} = k c_v T_{ad} = \frac{kR}{k-1} T_{ad} \quad (10)$$

Substituting (4), (9), and (10) into (3) yields

$$\dot{P}_{gH} x + k P_{gH} \dot{x} = \dot{m}_i \frac{kRT_{ad}}{A_g} \quad (11)$$

Although no detailed analyses of hydrogen peroxide decomposition were found, past experimental results indicate a pure time delay of 37 msec between monopropellant injection and decomposition [6]. Thus, the mass flow rate of hot gas into the hot gas cylinder is approximated as the mass flow of monopropellant through the solenoid valve,  $\dot{m}_{HP}$ , shifted by a delay time,  $\tau$ .

$$\dot{m}_i(t) = \dot{m}_{HP}(t - \tau) \quad (12)$$

By combining (11) and (12) and reordering terms, the equation for the hot gas dynamics is produced.

$$\dot{P}_{gH}(t) = \frac{1}{x(t)} \left( \frac{\dot{m}_{HP}(t - \tau) kRT_{ad}}{A_g} - k P_{gH}(t) \dot{x}(t) \right) \quad (13)$$

The dynamics of the mass flow of the monopropellant through the solenoid valve are estimated since there is no available data on specific valve dynamics other than the valve response time. The flow is modeled as a linear ramp to the steady state value over the valve response time.

As the gas in the high pressure hot gas cylinder expands, the gas in the low pressure hot gas cylinder is compressed. During the initial portion of the stroke, while the exhaust port is still uncovered, the low pressure hot gas cylinder is still open to atmosphere so its pressure is assumed to be equal to atmospheric pressure. Once the low pressure hot gas piston passes the exhaust port, the low pressure side behaves as an air spring. Assuming the process is adiabatic, the pressure of the low pressure side is found using the ideal gas equation of state.

Since the pressure drops across the hydraulic check valves are small compared to the changes in gas pressures and the high pressure hydraulic force,  $P_{fL}$  and  $P_{fH}$  are assumed to be constant with  $P_{fL}$  set to the hydraulic reservoir pressure and  $P_{fH}$  equal to the maximum load pressure of the fluid in the accumulator. Although the load pressure would vary in real applications, if the FPHP can pump against the maximum load, it is assumed that it can pump against all loads. Since there are no side loads on the FPA, the friction is not dependent on the

location of the FPA, as with a piston connected to a crankshaft, so  $F_{fric}$  is modeled as a constant.

## V. HARDWARE DESIGN

### A. High Temperature Sealing and Lubrication

The FPHP required the implementation of many novel design solutions in order to produce a functional prototype [8]. It was apparent from the beginning of the design process that the FPHP would need to function like an internal combustion (IC) engine mated to a piston hydraulic pump. Standard pneumatic piston/cylinder actuators can operate in conditions up to approximately 250°C. The FPHP had to withstand hydrogen peroxide decomposition gases at a temperature exceeding 700°C. Polymer seals and traditional petroleum lubricants combust at this temperature, so the technology used to construct a high temperature resistant piston/cylinder assembly was borrowed from IC engine design. Internal combustion engines use steel rings fitting in grooves on the hot gas piston to provide a seal against the bore of the cylinder, a design that reliably withstands peak combustion temperatures in excess of 2000°C [1]. This design archetype was adapted for use in the FPHP.

The hot gas pistons in an IC engine are usually made from aluminum while the cylinder bore is traditionally iron. This arrangement improves performance by reducing reciprocating mass and providing favorable wear characteristics between the piston and cylinder bore, since the softer aluminum wears in to the harder iron. Aluminum, however, has a coefficient of thermal expansion approximately 35% higher than iron. The hot gas piston must be designed with the appropriate diametrical clearance in the cylinder bore to avoid seizure at high temperatures. To estimate the required clearance, the circumference of a cylindrical object was assumed to expand linearly with increasing temperature. This assumption is valid for thin-walled cylinders in which the circumference is much greater than the thickness, since the amount of radial expansion of the wall is negligible compared to the circumferential expansion. For a thick-walled or solid cylinder (like the hot gas piston), the analysis may underestimate the amount of diametrical expansion since the radial thickness is not negligible. However, it is presumed that the assumption of linearity is adequately accurate for moderate temperature changes. Therefore, the change in length due to thermal expansion equals the product of the coefficient of expansion, the change in temperature, and the original length. The difference in the piston and cylinder diametrical expansions  $C_{dia}$  is given by

$$C_{dia} = (\alpha_p - \alpha_c) D \Delta T \quad (14)$$

where  $\alpha_p$  and  $\alpha_c$  are the linear thermal expansion coefficients for the piston and cylinder, respectively,  $D$  is the nominal bore of the cylinder and diameter of the piston, and  $\Delta T$  is the difference between the operating temperature of the FPHP and room temperature. Evaluating (14) under the FPHP operating conditions showed that the aluminum piston would expand approximately 0.08 mm (0.003 inches) more than the steel bore. The bore therefore was made about 0.13 mm (0.005 inches) larger than the piston at room temperature in order to maintain proper sliding clearance at operating temperature.

In addition to allowances for thermal expansion, the heat from the hot gases needed to be dissipated to avoid excessively high temperatures. Traditional IC engines use an oil-filled sump to provide a constant bath of oil to the wall of the cylinder. The FPHP could not be designed with an oil sump since it was comprised of the free piston geometry and had no crankcase to hold oil. Therefore, several unique ceramics were utilized to ensure adequate heat dissipation and lubrication. Thermal dispersant ceramic coating was applied to the exterior of the hot gas cylinder walls to improve heat dissipation, producing a black coloration. A dark gray lubricating ceramic layer was applied to both the hot gas piston sleeve and the hot gas cylinder bore. This ceramic coating reduced the friction between the two components and provided a very hard surface layer and longer wear life. A thermal barrier ceramic was applied to the hot gas piston heads to reduce heat conduction from the hot gases into the piston. Finally, solid lubricating powder was buffed onto the piston and cylinder bore contact areas.

### B. Alignment and Assembly

It was crucial to maintain a precise alignment of the hot gas and hydraulic cylinders to ensure smooth movement of the free piston assembly. Proper alignment was achieved by the use of press fit interfaces between the three cylinders. Fig. 3 shows a close up view of the press fit. A shoulder on the hot gas cylinder was pressed into the bore of the hydraulic cylinder with a light interference fit, ensuring that all three cylinders were concentric.

It was also necessary to assemble the hot gas piston concentrically with the connecting rod and hydraulic piston. A press fit in this location was infeasible since this would make disassembly very difficult. The hot gas piston also needed to withstand very high loads. The solution used was a conical bore in the hot gas piston that fit over a taper on the end of the connecting rod. The taper ensured a high level of concentricity and a large contact area between the hot gas piston and connecting rod to support high loads and prevent surface damage between the two. A crown nut preloaded the hot gas piston onto the connecting rod, as shown in Fig. 4. The crown nut was assembled with thread locking compound and safety wired onto the connecting rod to avoid loosening during high speed, high temperature operation.

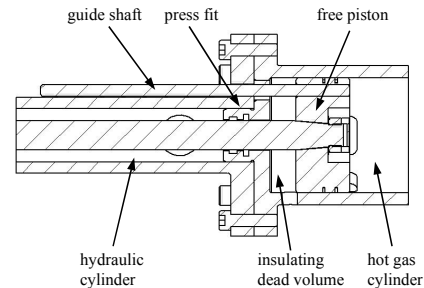


Figure 3: Press fit between hot gas and hydraulic cylinders.

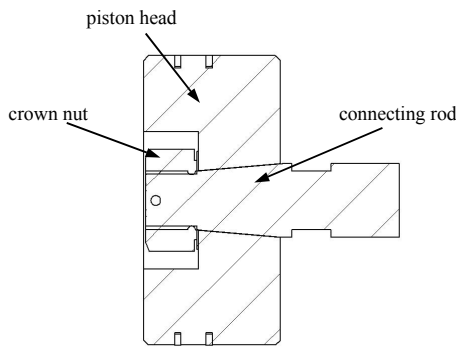


Figure 4: Cross-section view of hot gas piston assembly.

### C. Exhaust Port Design

The FPHP exploited the fact that a monopropellant does not require mixing with fresh air by eliminating intake ports and incorporating simple exhaust ports machined into the hot gas cylinder wall, which the hot gas piston uncovered at the end of each stroke. This feature allowed the hot gases to expand as much as possible before venting to the atmosphere. In contrast to traditional IC engines, there was no cam necessary to actuate exhaust valves as in four-stroke engines, nor proper timing to coordinate between the intake and exhaust ports as with two-stroke engines.

The use of exhaust ports in the hot gas cylinder wall necessitated the use of locking pins to prevent the rotation of the hot gas piston rings in their grooves. Should a ring rotate so that the seam of the ring passed over the exhaust port, the ring could spread into the port and catch on its edge, potentially seizing the piston within the bore. The locking pins were press fit into the ring groove, and each piston ring was notched at its ends to fit over the head of the locking pin and prevent rotation, as shown in Fig. 5. In a two-stroke IC engine, the piston itself is constrained from rotating by the connecting rod. The pistons in the FPHP needed to be constrained similarly to prevent the entire FPA from rotating. A guide shaft, shown in Fig. 3, was designed to be press fit into one of the hot gas pistons and passed through the base of the hot gas cylinder via a bronze bushing. The guide shaft, moving with the FPA, effectively constrained rotational motion of the piston assembly while allowing linear motion.

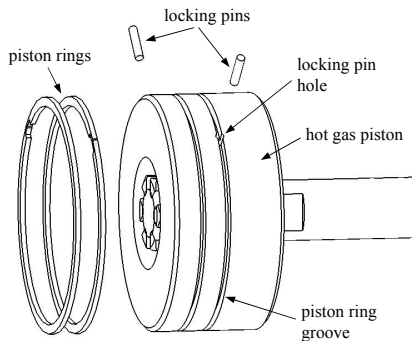


Figure 5: Exploded view of hot gas piston with locking pins.

### D. High Speed Hydraulics

The hydraulic piston required a seal to minimize fluid leakage between the piston and hydraulic cylinder bore.

Traditional hydraulic piston applications include large, slow moving devices such as backhoes and dump trucks. The seals used in these machines rarely experience piston speeds exceeding 1.0 m/s. Since the FPHP needed a seal capable of a maximum piston speed near 8.0 m/s, bronze-impregnated Teflon seals were chosen to perform at this level.

There was a significant pressure drop across the check valves that facilitated the pumping of the hydraulic fluid. Cavitation could occur during the intake of the fluid if the pressure drop across the check valve reduced the pressure of the fluid to its vapor pressure. A significant drop in pressure would also bring dissolved air out of solution in the hydraulic fluid, producing more bubbles. The hydraulic fluid would become much more compressible if it contained many bubbles in suspension. On the intake stroke, the pressure forcing the fluid through the check valve was only atmospheric pressure, so a pressure drop of approximately 1.0 atm (15 psi) produced cavitation. The solution to this problem was to pressurize the reservoir above atmospheric pressure to prevent the hydraulic fluid from dropping to below its vapor pressure at the inlet of the FPHP. This technique enabled the use of a more compact check valve while avoiding cavitation. Pressurizing the reservoir to 310 kPa (45 psi) eliminated cavitations under all circumstances.

### E. Experimental Hardware

The following figures depict various aspects of the prototype FPHP system. Fig. 6 shows a photograph of the main components of the FPHP before assembly. Fig. 7 shows the FPHP system with the main components labeled. A detailed description of the experimental verification of the FPHP is presented in [7] and [8].

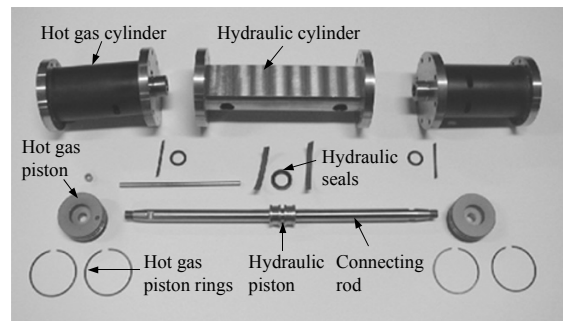


Figure 6: FPHP hardware.

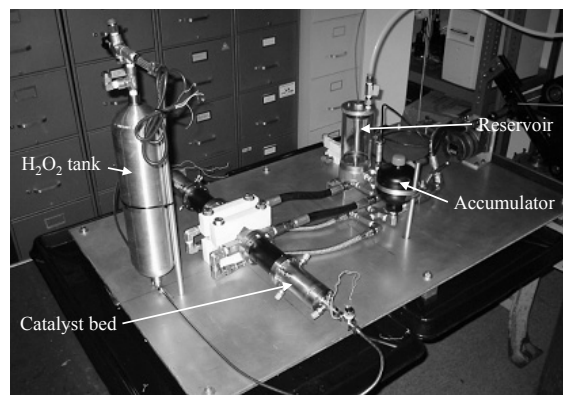


Figure 7: FPHP system.

## VI. SPECIFIC POWER AND SPECIFIC ENERGY

### A. Ragone Plot

Once the dynamics and design of the FPHP were determined, its performance was assessed using a Ragone plot. Ragone plots portray the specific power of a system versus its specific energy for a large range of operation times. The specific energy and specific power of a power supply system must be expressed as parametric functions of time in order to graph the system's performance on a Ragone plot. The specific energy  $\hat{E}$  is expressed by

$$\hat{E} = \frac{E_{tot}}{m_{sys}} = \frac{Pt}{m_{fuel} + m_{tank} + m_{eng}} \quad (15)$$

where  $E_{tot}$  is the total energy required for the operating time  $t$  of the system,  $m_{sys}$  is the total system mass including the mass of the fuel  $m_{fuel}$ , fuel tank  $m_{tank}$ , and engine  $m_{eng}$ , and  $P$  is the rated power. The weight of the actuators, accumulator, reservoir, and the framework to hold the main components together was neglected since the systems compared would share similar components. The mass of the fuel is

$$m_{fuel} = \frac{E_{tot}}{\eta_{sys} \hat{h}} \quad (16)$$

where  $\hat{h}$  is the specific energy of the fuel and  $\eta_{sys}$  is the system efficiency converting fuel to hydraulic energy. The system efficiency is the product of efficiencies for each energy transformation of the system, for example from electrical power to shaft power at the motor to hydraulic power at the pump for an electro-hydraulic system. The fuel tank mass was assumed to scale linearly with the fuel mass.

$$\beta = \frac{m_{fuel}}{m_{tank}} \quad (17)$$

Therefore, the mass of the fuel tank is

$$m_{tank} = \frac{m_{fuel}}{\beta}. \quad (18)$$

Using (16) – (18) in (15) and simplifying produces

$$\hat{E} = \left[ \frac{1}{\eta_{sys} \hat{h}} \left( 1 + \frac{1}{\beta} \right) + \frac{m_{eng}}{Pt} \right]^{-1}. \quad (19)$$

Similarly, the specific power  $\hat{P}$  is

$$\hat{P} = \frac{P}{m_{sys}} = \frac{\hat{E}}{t}. \quad (20)$$

Therefore, for a given operating time, one point  $(\hat{E}(t), \hat{P}(t))$  is generated on the Ragone plot for each power system. The diagonal lines correspond to constant operating times on a logarithmic scale.

### B. Parameter Estimation

The Ragone plot, shown in Fig. 8, was used to compare the FPHP to two other hydraulic power supplies capable of anaerobic operation. The first consists of batteries powering an electric motor coupled to a rotary hydraulic pump, the other is of a device similar to the FPHP using hydrazine ( $N_2H_4$ ), a common aerospace monopropellant, instead of hydrogen peroxide. Table 1 shows the values of the parameters used in creating the Ragone plot. Each power system was scaled for a hydraulic power output of 2.2 kW, although the results are scalable for a range of power outputs. The performance of the systems in Fig. 8 must be taken as approximate since the efficiency and mass of the systems were estimated when necessary rather than calculated or measured. The simulation in [7] provided the performance values (power and conversion efficiency) necessary to evaluate the theoretical performance of the FPHP with a Ragone plot. Pure hydrogen peroxide was used as the monopropellant for the FPHP in Fig. 8. The mass of the FPHP was estimated assuming primarily aluminum construction for weight savings instead of the stainless steel prototype version. The fuel storage ratio  $\beta$  was estimated by dividing the mass of a given volume of fuel by the mass of a commercial carbon fiber storage tank capable of holding that fuel.

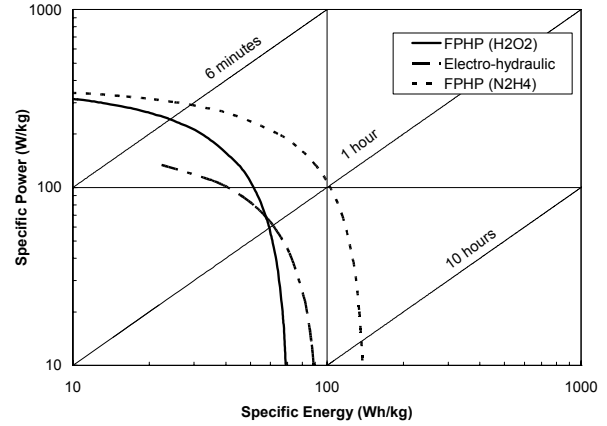


Figure 8: Ragone plot power sources.

TABLE I. PARAMETER VALUES USED FOR RAGONE PLOT

	FPHP ( $H_2O_2$ )	Electro-hydraulic	FPHP ( $N_2H_4$ )
$\eta_{sys}$	0.20	0.64	0.20
$\beta$	3.9	--	2.7
$m_{eng}$	6 kg	12.5 kg	6 kg
$\hat{h}$	1.6 MJ/kg	0.53 MJ/kg	3.5 MJ/kg

The electro-hydraulic system has no fuel tank mass ( $1/\beta = 0$ ) but is limited for short operating times by the

maximum specific power of the batteries, thus no points could be generated for battery masses below the minimum needed to produce the desired power. Typical performance specifications were used for electric motor and hydraulic pump efficiencies (80% for electric to shaft power, 80% for shaft to hydraulic power, producing a system efficiency of 64%). The batteries were assumed to be high-performance lithium ion, with a specific energy of 529 kJ/kg and specific power of 420 W/kg [11]. The specific power of a DC motor coupled to a hydraulic pump was estimated to be 220 W/kg, producing a 12.5 kg actuator for a required shaft power of  $(2200 \text{ W}) / 0.8 = 2750 \text{ W}$ .

It is evident that the FPHP system is not a practical power supply in its current form except perhaps for short applications less than one hour. Fig. 8 shows another monopropellant system powered by hydrazine, which has a specific energy of 3.5 MJ/kg. Assuming similar efficiency values for an FPHP-type device using this monopropellant, the projected performance is plotted alongside the hydrogen peroxide FPHP and the electro-hydraulic system. A successful hydrazine powered system could outperform the two other systems for a large range of operating times. Fig. 9 shows the initial system mass for various operating times of the three chosen power sources. The mass of the electro-hydraulic system would remain constant throughout the operating time, but the other two systems would become lighter as the monopropellant was consumed.

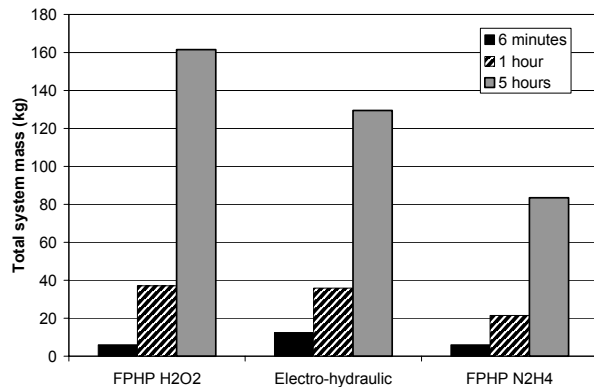


Figure 9: System mass for various operating times.

## VII. CONCLUSIONS

The Free Piston Hydraulic Pump (FPHP) represents a new concept for a power supply for mobile robotic applications, integrating a monopropellant-based system with a free piston pump. Monopropellants cannot compete with hydrocarbon fuels for most air-breathing applications, but they do provide a possible solution for a free piston anaerobic power source. Hydrogen peroxide provides inadequate specific energy to make the FPHP a feasible concept for a hydraulic power supply, but a monopropellant with a greater specific energy may make the FPHP desirable for certain anaerobic applications.

## REFERENCES

- [1] Heywood, J.B., *Internal Combustion Engine Fundamentals*, McGraw-Hill, New York, NY, 1988.
- [2] Tikkanen, S. and Vilenius, M., "On the Dynamic Characteristics of the Hydraulic Free Piston Engine," Proc. 2<sup>nd</sup> Tampere International Conference on Machine Automation, Tampere, Finland, 1998.
- [3] Heintz, R.P., "Theory of Operation of a Free Piston Engine-Pump," SAE paper #859316, 1985.
- [4] Beachley, N.H. and Fronczak, F.J., "Design of a Free-Piston Engine-Pump," SAE paper #921740, 1992.
- [5] Achten, P.A.J., "A Review of Free Piston Engine Concepts," SAE paper #941776, 1994.
- [6] Barth, E.J., Gogola, M.A., Wehrmeyer, J.A., Goldfarb, M., "The Design and Modeling of Liquid-Propellant-Powered Actuator for Energetically Autonomous Robots," Proc. ASME International Mechanical Engineering Congress & Exposition, New Orleans, LA, 2002.
- [7] McGee, T.G., Raade, J.W., Kazerooni, H., "Theoretical Analysis and Experimental Verification of a Monopropellant-Driven Free Piston Hydraulic Pump," *ASME J. Dyn. Sys., Meas., and Control*, in press.
- [8] Raade, J.W., McGee, T.G., Kazerooni, H., "Design, Construction, and Experimental Evaluation of a Monopropellant Powered Free Piston Hydraulic Pump," Proc. ASME International Mechanical Engineering Congress & Exposition, Washington, D.C., 2003.
- [9] Ragone, D.V., "Review of Battery Systems for Electrically Powered Vehicles," SAE paper #680453, 1968.
- [10] Schumb, W.C., Satterfield, C.N., Wentworth, R.L., *Hydrogen Peroxide*, Reinhold Publishing, New York, NY, 1955.
- [11] Duke, M., "Solion Li-ion Battery System for Solar Racing Cars," Solion Limited, <http://www.lsbu.ac.uk/solarcar/solion.pdf>, accessed on February 26, 2004.